Hindawi Publishing Corporation
International Journal of Photoenergy
Volume 2013, Article ID 567426, 7 pages
http://dx.doi.org/10.1155/2013/567426

Research Article

Photoelectrocatalytic Performance of Benzoic Acid on TiO_2 Nanotube Array Electrodes

Hongchong Chen, Jinhua Li, Quanpeng Chen, Di Li, and Baoxue Zhou

School of Environmental Science and Engineering, Shanghai Jiao Tong University, Shanghai 200240, China

Correspondence should be addressed to Baoxue Zhou; zhoubaoxue@sjtu.edu.cn

Received 4 February 2013; Revised 22 April 2013; Accepted 22 April 2013

Academic Editor: Jiaguo Yu

The photoelectrocatalytic performance of benzoic acid on TiO_2 nanotube array electrodes was investigated. A thin-cell was used to discuss the effect of the bias voltage, illumination intensity, and electrolyte concentration on the photoelectrocatalytic degradation efficiency of benzoic acid. The photogenerated current-time (I-t) profiles were found to be related to the adsorption and the degradation process. The relationship between the initial concentration and the photocurrent peaks (I_{0ph}) fits the Langmuir-type adsorption model, thus confirming that the adsorption of benzoic acid on TiO_2 nanotube arrays (TNAs) was single monolayer adsorption. At low concentrations, the I-t profiles simply decay after the initial transient peak due to the sufficient holes on the TNAs which would oxidize the benzoic acid quickly. However, the I-t profiles varied with increasing benzoic acid concentrations because the rate of diffusion in the bulk solution and the degradation of the intermediate products affect the photoelectrocatalysis on the electrode surface.

1. Introduction

For nearly three decades, the photocatalytic and photoelectrocatalytic degradation of organic substances on wide-bandgap semiconductive TiO_2 nanomaterials have drawn considerable attention because of their high photocatalytic efficiency, nontoxicity, nonphotocorrosiveness, favorable biological and chemical inertness, and low cost [1–5]. However, conventional TiO_2 nanoparticles also exhibit defects such as a high electron-hole recombination rate, low photocatalytic degradation efficiency, and difficult follow-up process [6].

To overcome these defects, considerable effort has been devoted to improving the photocatalytic ability of TiO_2 catalysts, including the synthesis of new TiO_2 structures [7–11]. TiO_2 nanotube arrays (TNAs) have gained attention and have been successfully applied to the photoelectrocatalytic degradation of a variety of organic pollutants because of their peculiar architecture, large surface area, high adsorption capacity, easy teleportation, and highly efficient degradation of organics [12–15].

Traditional studies on the photoelectrocatalytic oxidation of organic compounds were mainly performed in bulk reactors, wherein the pollutant concentration was repeatedly determined over a certain period via absorption spectrophotometry [16–18]. However, this method limits the in-depth investigation of the reaction mechanism because of the relatively large body solution and long diffusion channel [19]. The use of a thin-cell with a small-volume cavity facilitated the study of the adsorption characteristics of organic substances and their interactions with the catalyst because of the subsequent increase in the ratio of the photoanode area to the organic solution volume. These studies led to the rapid completion of the exhaustive redox reaction [19, 20].

Benzoic acid was typical aromatic ring acid compound. It was the most commonly used food preservative and antibacterial agent [21]. It was also extensively used in the printing and dyeing industry (as a mordant of dyeing and printing) as well as in the pharmaceutical (as the intermediate) [22], steel (as an antirust agent) [23], and other industries [24]. In addition, benzoic acid is the intermediate metabolic product of various aromatic compounds and also the degradation intermediate product of many complex refractory organics [25]. However, few reports on the photoelectrocatalytic performance of benzoic acid compounds have been released.

In this paper, the photoelectrocatalytic performance of benzoic acid on TNA electrodes was investigated using a thin-cell reactor. The adsorption properties, microcosmic degradation process, and reaction characterization of benzoic acid on TNAs were investigated by analyzing the change in the photogenerated current-time (I_{ph}-t) profiles. The result of this study provides a solid foundation for future research into the reaction mechanism and reaction kinetics of aromatic organic compounds on TNA electrode surfaces.

2. Materials and Methods

2.1. Materials. Titanium sheets (0.25 mm thick, 99.9% purity) were purchased from Sumitomo Chemical (Japan). Unless otherwise indicated, reagents were obtained from Sinopharm Chemical Reagent Company and were used as received. High-purity deionised water was used in the preparation of all solutions.

2.2. Preparation of TiO_2 Nanotube Array Electrode. The preparing method of TiO_2 nanotube array electrodes has been published in our previous work [18]. Hence, only key points of the fabrication process were summarized here. The electrolyte contain 0.1 mol/L NaF, 1 mol/L $NaHSO_4$ and 0.2 mol/L trisodium citrate, also with NaOH added to adjust the pH. The TiO_2 nanotube array electrodes are prepared under constant stirring for 4 h. After anodization, the as-prepared sample was washed with high-purity deionized water and dried at room temperature. Then it was annealed in a laboratory muffle furnace at 500°C to crystallize in the air ambience. X-ray diffraction (Bruker, D8 ADVANCE, Germany) analysis showed that the crystal structure of TNA is anatase [18].

2.3. Apparatus and Methods. All experiments were performed at room temperature in a three-electrode electrochemical cell with a quartz window (0.82 cm^2). The thickness of the spacer was 0.1 mm, which defined the cell volume of 8.2 μL. The structure of thin-cell reactor has been reported in our previous paper [18]. The TiO_2 nanotube array electrode was used as a working electrode; a saturated Ag/AgCl electrode and a platinum foil were used as the reference and the counter electrodes, respectively. Also 2 mol/L $NaNO_3$ was chosen as the supporting electrolyte in the experiment. The supply bias and work current are controlled by a CHI (CH Instrument, Inc., CHI601d, USA) electrochemical analyzer; 2W LED UV lamp (365 nm) was chosen as UV light source. The light intensity in experiment was measured by UV-A ultraviolet irradiator.

3. Results and Discussion

3.1. The Photocurrent-Time Profile Property and Net Charge Determined in Thin-Cell. In the photoelectrochemical reaction, the oxidation of organic compounds at the electrodes can be represented by the following electrode reaction equation:

$$\begin{aligned} C_yH_mO_jN_kX_q + (2y - j)\,H_2O \\ \longrightarrow y CO_2 + qX^- + kNH_3 \\ + (4y - 2j + m - 3k)\,H^+ \\ + (4y - 2j + m - 3k - q)\,e^-, \end{aligned} \tag{1}$$

where X represents the halogen atom. The numbers of carbon, hydrogen, oxygen, nitrogen, and halogen atoms in the organic compound are represented by y, m, j, k, and q.

Faraday's law can be used to quantify the concentration by measuring the charge passed if the organics is completely oxidized. That is,

$$Q_{net} = \int I\,dt = nFVC, \tag{2}$$

where I is the photocurrent from the oxidation of the organics and t is the time elapsed upon illumination; Q_{net} is the direct measure of net charge of the organics; n is the number of electrons transferred and C is the concentration of the organics, while the volume (V) and the Faraday constant (F) are known constants.

Figure 1 shows a set of typical photocurrent-time profiles in the exhaustive mode in thin-cell at the fixed applied bias potential of 2.5 V. Figures 1(c) and 1(d) show the photocurrent response of a blank solution of 2.0 mol/L $NaNO_3$ and a 2.0 mol/L $NaNO_3$ solution containing 0.4 mmol/L benzoic acid in a thin-cell in the absence of illumination (electrocatalytic performances). The results show that there is no photocurrent under dark conditions which indicate that the benzoic acid in thin-cell cannot be oxidized. Figure 1(a) shows the typical photocurrent response of a blank solution of 2.0 mol/L $NaNO_3$ under the illumination conditions (7.9 mW/cm^2). The even photocurrent (I_{blank}) observed for the blank solution originated from the stable oxidation of water. Figure 1(b) shows the photocurrent response of a 2.0 mol/L $NaNO_3$ solution containing 0.4 mmol/L benzoic acid in a thin-cell under the same illumination (7.9 mW/cm^2). The total photocurrent (I_{total}) observed for the benzoic acid solution was the total of two different components: one originates from the photoelectrocatalytic oxidation of benzoic acid, whereas the other was from water oxidation, which was the same as I_{blank} (Figure 1(a)). When the I_{total} decreases to the level of I_{blank}, the oxidation of organics was finished. Hence, the processes of the photoelectrochemical reaction in thin-cell were described by the change of I-t profile.

The net charge which originated from the oxidation of organics was defined as Q_{net}, which can be obtained by subtracting Q_{blank} from Q_{total}. The net charge which obtained by (2) was defined as ThQ_{net}. Because the change of net charge is directly related to concentration of organics during the photoelectrochemical reaction. The degradation efficiency (DE) of the photoelectrochemical reaction can be defined as the ratio of Q_{net} to ThQ_{net}, which can be used in describing the property of thin-cell.

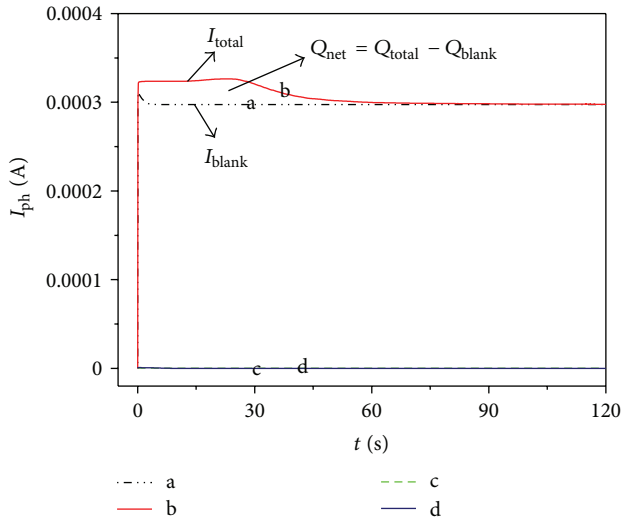

Figure 1: Typical photocurrent-time responses obtained from the thin-cell (a) 2.0 mol/L $NaNO_3$ solution under illumination; (b) 2.0 mol/L $NaNO_3$ with 0.4 mmol/L benzoic acid under illumination; (c) 2.0 mol/L $NaNO_3$ solution under no illumination; (d) 2.0 mol/L $NaNO_3$ with 0.4 mmol/L benzoic acid under no illumination.

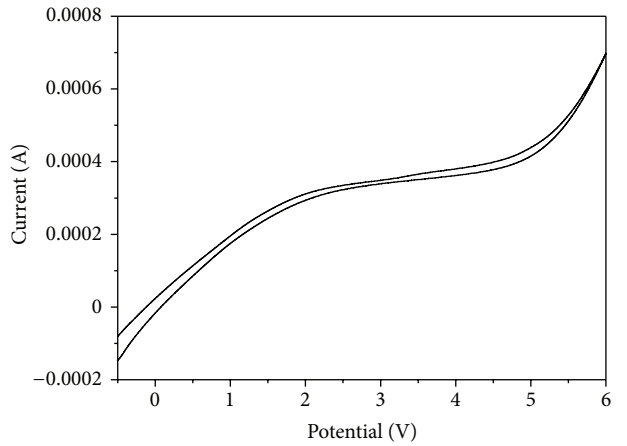

Figure 2: Cyclic voltammograms of a 2.0 mol/L $NaNO_3$ blank solution in a thin-cell reactor based on the TNA electrodes under illuminations of 7.9 mW/cm^2.

According to (1), the stoichiometric oxidation of benzoic acid can be represented as

$$C_7H_6O_2 + 12H_2O \longrightarrow 7CO_2 + 30H^+ + 30e^-. \quad (3)$$

That is, if the complete mineralisation of benzoic acid has been achieved, 1 mol of benzoic acid requires 30 mol of electrons. The relationship between the net charge and the concentration should be written as follows with the cell volume, $V = 8.2\,\mu$L, being used:

$$ThQ_{net} = 30FVC = 0.0237C. \quad (4)$$

Hence, the ThQ_{net} of 0.2 mmol/L, 0.4 mmol/L, and 0.8 mmol/L were 0.00474 mC, and 0.00948 mC, 0.01896 mC.

3.2. Effect of Photoelectrocatalytic Degradation on Benzoic Acid

3.2.1. Effect of the Bias Voltage. The cyclic voltammograms of a 2.0 mol/L $NaNO_3$ solution is shown in Figure 2. The photocurrent increases with the bias voltage, indicating that the bias voltage can improve the electronic transmission performance of TNAs in the thin-cell. This increase may affect the photoelectrocatalytic degradation efficiency of benzoic acid. In the low-bias voltage range (<2 V), the photocurrent rapidly increases with the bias voltage, thus demonstrating that the photogenerated electrons cannot be completely exported to the external circuit. When the bias voltage is between 2 and 4 V, the photocurrent appears in a saturated platform, indicating that the photogenerated electrons have been completely exported and that the recombination of electrons and holes has been restricted. After the platform becomes saturated (>4 V), the photocurrent again increases with the bias voltage and can cause the water molecules to decompose when the bias voltage reaches the oxygen evolution potential of the TNA electrode. The results in Figure 3 support this view.

Figure 3 shows the photocurrent-time profile of benzoic acid (0.4 mmol/L) degradation at different bias voltages and under 7.9 mW/cm^2 ultraviolet (UV) illuminations. As show in Figure 3, when the bias voltage is below 3 V, the degradation time of benzoic acid decreased as the bias voltage increased. This was indicated that the increase in the bias voltage can also improve the degradation rate of benzoic acid on TNAs. However, the photocurrent curve continuously increases when the bias voltage is 4 V, which leads to failure in identifying the reaction termination using a computer. This result indicates that the degradation of benzoic acid is significantly perturbed by the water decomposition when the bias voltage is too high.

Table 1 shows the Q_{net} value and degradation efficiency (DE) of benzoic acid under different bias voltages. When the bias voltage is below 2 V, the DE of benzoic acid increases with the bias voltage, indicating that the application of a bias voltage can enhance the photoelectrocatalytic capability of TNAs for benzoic acid. When the bias voltage is set between 2 and 3 V, the degradation efficiency of benzoic acid exceeds 99.5%, indicating that the benzoic acid is completely degraded. The Q_{net} value remains stable in this condition, indicating that the value of Q_{net} is related only to the transferred electronics during the photoelectrocatalytic oxidation. Therefore, the bias voltage should be set within the electrochemical window (2 V to 3 V).

3.2.2. Effect of Light Intensity. Figure 4 shows the photocurrent responses of a 2 mol/L $NaNO_3$ blank solution containing benzoic acid (0.4 mmol/L) under different light intensities. The more intense the light, the shorter the time for complete degradation, indicating that an increase in the intensity of light is conducive to promoting the photoelectrocatalytic degradation rate.

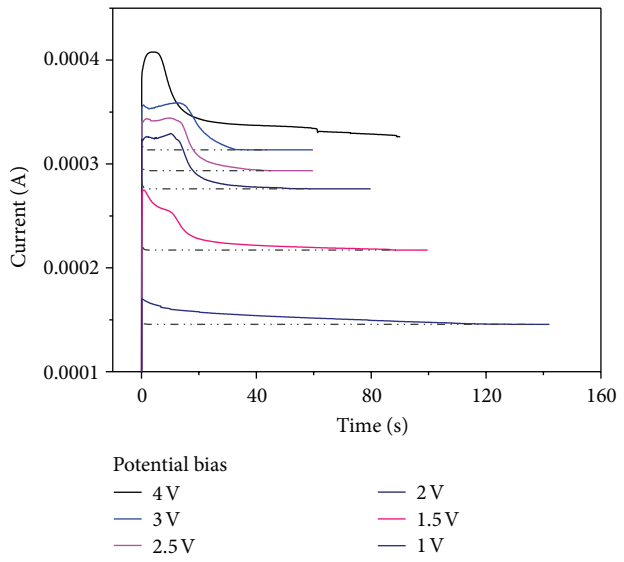

Figure 3: Photocurrent responses of a 2 mol/L $NaNO_3$ blank solution containing benzoic acid (0.4 mmol/L) in the thin-cell reactor based on the TNA electrodes at different fixed applied bias potentials under bias voltages under illuminations of 7.9 mW/cm^2.

Figure 4 shows that the photocurrent increases with the light intensity, indicating that the increases of light intensity can improve the electronic transmission performance of TNAs. The photocurrent-time curve shapes vary with the light intensity, demonstrating that the light intensity affects the photoelectrocatalysis of benzoic acid on TNAs.

Table 2 shows that the Q_{net} and degradation efficiency of 0.8 mmol/L benzoic acid increase with the light intensity when the light intensity is below 5.53 mW/cm^2. This result indicates that benzoic acid is not completely mineralized because of the insufficient light intensity not inducing enough electron-hole pairs of TNAs in the thin-cell.

However, the Q_{net} of benzoic acid at low concentrations (0.2 and 0.4 mmol/L) and at 0.8 mmol/L under sufficient light intensity (above 5.53 mW/cm^2) remain comparatively constant, confirming that Q_{net} is not related to the light intensity but is associated with the transferred electrons in the photoelectric catalytic oxidation when benzoic acid is completely mineralized.

3.2.3. Effect of Electrolyte Concentration. The transfer of electrons in the thin-cell reactor was affected by the electrolyte solution. The voltammograms of 0.4 mmol/L benzoic acid with different $NaNO_3$ concentrations under light (7.9 mW/cm^2) are shown in Figure 5. The photocurrent rapidly increases with the voltage when the $NaNO_3$ concentration is below 1 mol/L, indicating that the photoinduced electrons are not completely exported to the external circuit. When the concentration exceeds 1.5 mol/L, the photocurrent exhibits a saturated platform, indicating that the photogenerated electrons are completely exported and that the recombination of electrons and holes is restricted. The higher the electrolyte concentration, the stronger the conductivity.

Table 1: Q_{net} value and degradation efficiency (DE) under different bias voltages.

Bias voltage (V)	1	1.5	2	2.5	3
Q_{net} (mC)	0.008511	0.009048	0.009433	0.009469	0.009443
DE (%)	90.20	95.45	99.50	99.88	99.61

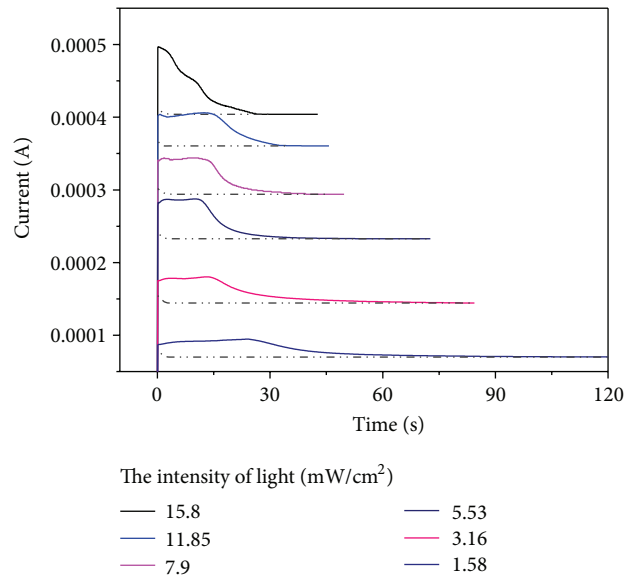

Figure 4: Photocurrent responses of a 2 mol/L $NaNO_3$ blank solution containing benzoic acid (0.4 mmol/L) in the thin-cell reactor based on the TNA electrodes at the fixed applied bias potential of 2.5 V under different light intensities.

Table 3 shows that Q_{net} gradually increases with the electrolyte concentration and is lower than ThQ_{net} when the $NaNO_3$ electrolyte concentration is below 1 mol/L. These results indicate that benzoic acid cannot be completely degraded because of the insufficient number of hole on TNAs. When the $NaNO_3$ electrolyte concentration exceeds 1.5 mol/L, Q_{net} remains stable and close to ThQ_{net}, indicating that benzoic acid has been completely degraded because of the sufficient number of holes in this condition.

3.3. Photoelectrocatalytic Degradation Property and Mechanism of Benzoic Acid. The photocurrent response profiles of benzoic acid for seven different concentrations in the thin-cell reactor are shown in Figure 6. A comparison between Q_{net} and ThQ_{net} shows that the different concentrations of benzoic acid have all been completely degraded in a photoelectrocatalytic manner.

The relationship between the initial organic concentrations and I_{0ph} was used to analyze the adsorption properties of benzoic acid on TNAs because the I_{0ph} value corresponds to the initial degradation rate according to the principle of photoelectric catalysis. Figure 6(a) shows that the peak photocurrent (I_{0ph}) increases with C_0. At low organic concentrations, I_{0ph} is proportional to C_0, possibly because of the photohole capture process during benzoic acid mineralization. However, as the benzoic acid concentration

Table 2: Q_{net} value and degradation efficiency (DE) of different concentrations of benzoic acid under varying light intensities.

Concentration (mmol/L)	Light intensities (mW/cm^2)	1.58	3.16	5.53	7.9	11.85	15.8
0.2	Q_{net} (mC)	0.009423	0.009434	0.009421	0.009467	0.009449	0.009409
	DE (%)	99.47	99.52	99.38	99.86	99.67	99.25
0.4	Q_{net} (mC)	0.009471	0.009454	0.009513	0.009470	0.009406	0.009433
	DE (%)	99.90	99.72	100.34	99.89	99.21	99.50
0.8	Q_{net} (mC)	0.008552	0.009075	0.009434	0.009445	0.009466	0.009429
	DE (%)	90.21	95.73	99.52	99.63	99.85	99.46

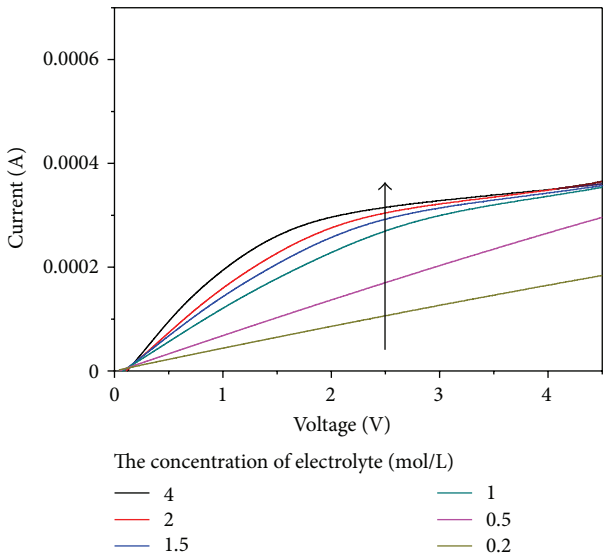

Figure 5: Voltammograms of different concentrations of $NaNO_3$ blank solution containing benzoic acid (0.4 mmol/L) in the thin-cell reactor based on the TNA electrodes under illumination of 7.9 mW/cm^2.

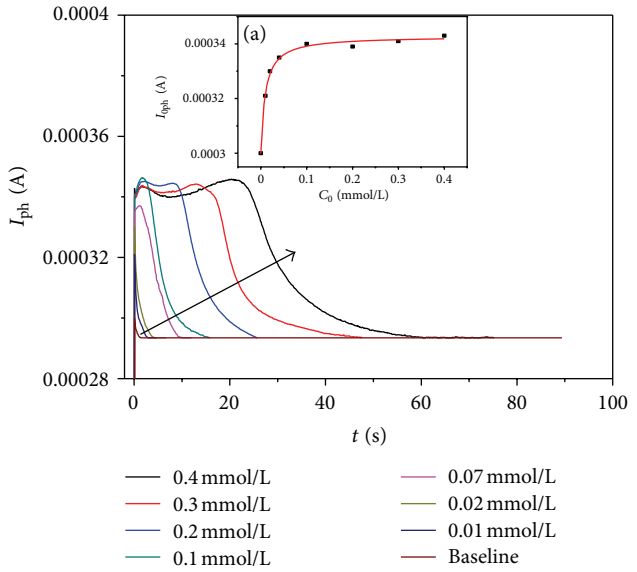

Figure 6: Photocurrent response profiles derived from the photoelectrocatalytic oxidation of different concentrations of benzoic acid in the thin-cell reactor based on the TNA electrodes. (a) Relationship between the initial concentration (C_0) and the net peak photocurrent (I_{0ph}) of the TNA electrode for benzoic acid.

Table 3: Q_{net} and degradation efficiency of 0.4 mmol/L benzoic acid with different $NaNO_3$ concentrations under illumination of 7.9 mW/cm^2 and a fixed applied bias voltage of 2.5 V.

Electrolyte concentration (mol/L)	0.5	1	1.5	2
Q_{net} (mC)	0.008112	0.009260	0.009415	0.009436
DE (%)	85.57	97.68	99.31	99.54

increases to a certain level, photohole generation becomes the rate-limiting step, and the increase in I_{0ph} begins to slow down.

The relationship between I_{0ph} and C_0 was simulated using a computer as follows:

$$I_{0ph} = \frac{4 \times 10^{-5} \times 106C_0}{1 + 106C_0} + 0.0003, \qquad R^2 = 0.9945. \quad (5)$$

The data (4) fit the *Langmuir* adsorption isotherm. These results confirm that the adsorption behavior of benzoic acid on the TNAs is that of a monolayer adsorption.

The photocurrent response profiles of benzoic acid at seven different concentrations are shown in Figure 6. The degradation *I-t* profiles all show decay to a stable value. However, this decay varies with increasing concentrations, thereby illustrating the disparities in the photoelectrocatalytic process as well as the mechanism of benzoic acid degradation at different concentrations.

At low concentrations (0 mmol/L to 0.02 mmol/L), the transient photocurrent rapidly reaches its peak at the initial stage because of the rapid degradation of the benzoic acid originally adsorbed on the TNA surface. The photocurrent then begins to decrease because of benzoic acid mineralization. After a certain period, the photocurrent finally reaches a stable value and overlaps with I_{blank}. This result indicates that the photoelectrocatalytic degradation of benzoic acid in the thin-cell reactor is complete.

When the benzoic acid concentration reaches an intermediate level (0.07 mmol/L to 0.1 mmol/L), the curve continues increasing after the initial peak, possibly because of the

degradation of the intermediates. Figure 6(a) shows that the adsorption of the electrode surface has not reached saturation at that point, indicating that the number of photogenerated holes on the electrode surface is sufficient. Thus, the rapid oxidation of intermediate products, which can be more easily oxidized than benzoic acid, may have caused the current to increase.

As the concentration increases to levels above 0.2 mmol/L (0.1 mmol/L, e.g.), the *I-t* profiles can be divided into five major processes: a rapid increase to the transient photocurrent spikes, a continuous increase, a rapid decrease, a reincrease, and a decrease to a stable value. Meanwhile, Figure 6(a) shows that the adsorption on the TNAs has reached saturation, indicating that the holes on the TNA electrode surface cannot oxidate all benzoic acid on the TNAs simultaneously. This photoelectrocatalytic process can be explained as follows. In the initial stage, the benzoic acid molecule on the surface of the TNA electrode is rapidly oxidized, and the photocurrent rapidly reaches the initial peak. After the first oxidization, the resting benzoic acid absorbed on the TNA surface at elevated concentrations as well as the intermediate products is oxidized, which results in the continuous increase of the curve for benzoic acid after the initial peak. The benzoic acid concentration cannot be supplemented in time because the rate of adsorption may be slower than the speed of degradation. Therefore, the optical current rapidly decreases. After a certain period, the area covered by the benzoic acid absorbents begins to increase, which results in a re-increase in the current. Afterward, the benzoic acid concentration decreases, which results in the decrease in the photocurrent. These findings indicate that when the benzoic acid concentration is high, the diffusion of benzoic acid in the bulk solution of the reactor as well as the degradation of intermediate products from benzoic acid decomposition would affect the photoelectrocatalysis on the electrode surface.

4. Conclusions

The photoelectrocatalytic performance of benzoic acid on the TiO_2 nanotube array electrode was investigated using a thin-cell reactor. The adsorption, degradation rate, and reaction characteristics of benzoic acid degradation were discussed by analyzing the changes in the photogenerated *I-t* profiles. The result of this paper provides a solid foundation for future research into the degradation characteristics, reaction mechanism, and reaction kinetics of aromatic organic compounds on the TNA electrode surface.

Acknowledgments

The project was supported by the National High Technology Research and Development Program of China (863) (2009AA063003), the National Natural Science Foundation of China (no. 20 677039), and R&D Foundation of Shanghai Jiaotong University. The authors are for support of XRD lab in Instrumental Analysis Center of SJTU.

References

[1] J. H. Carey, J. Lawrence, and H. M. Tosine, "Photodechlorination of PCB's in the presence of titanium dioxide in aqueous suspensions," *Bulletin of Environmental Contamination and Toxicology*, vol. 16, no. 6, pp. 697–701, 1976.

[2] D. H. Kim and M. A. Anderson, "Photoelectrocatalytic degradation of formic acid using a porous TiO_2 thin-film electrode," *Environmental Science and Technology*, vol. 28, no. 3, pp. 479–483, 1994.

[3] X. Z. Li, H. L. Liu, P. T. Yue, and Y. P. Sun, "Photoelectrocatalytic oxidation of rose Bengal in aqueous solution using a Ti/TiO_2 mesh electrode," *Environmental Science and Technology*, vol. 34, no. 20, pp. 4401–4406, 2000.

[4] H. L. Liu, D. Zhou, X. Z. Li, and P. T. Yue, "Photoelectrocatalytic degradation of Rose Bengal," *Journal of Environmental Sciences*, vol. 15, no. 5, pp. 595–599, 2003.

[5] S. Dezhl, C. Sheng, J. S. Chung, D. Xiaodong, and Z. Zhibin, "Photocatalytic degradation of toluene using a novel flow reactor with Fe-doped TiO_2 catalyst on porous nickel sheets," *Photochemistry and Photobiology*, vol. 81, no. 2, pp. 352–357, 2005.

[6] J. Bai, J. H. Li, Y. B. Liu, B. X. Zhou, and W. M. Cai, "A new glass substrate photoelectrocatalytic electrode for efficient visible-light hydrogen production: CdS sensitized TiO_2 nanotube arrays," *Applied Catalysis B*, vol. 95, no. 3-4, pp. 408–413, 2010.

[7] Y. X. Li, Y. Xiang, S. Q. Peng, X. W. Wang, and L. Zhou, "Modification of Zr-doped titania nanotube arrays by urea pyrolysis for enhanced visible-light photo electrochemical H_2 generation," *Electrochimica Acta*, vol. 87, no. 1, pp. 794–800, 2013.

[8] D. W. Gong, C. A. Grimes, O. K. Varghese et al., "Titanium oxide nanotube arrays prepared by anodic oxidation," *Journal of Materials Research*, vol. 16, no. 12, pp. 3331–3334, 2001.

[9] Z. H. Xu and J. G. Yu, "Visible-light-induced photoelectrochemical behaviors of Fe-modified TiO_2 nanotube arrays," *Nanoscale*, vol. 3, no. 8, pp. 3138–3144, 2011.

[10] G. P. Dai, J. G. Yu, and G. Liu, "Synthesis and enhanced visible-light photoelectrocatalytic activity of p-N junction $BiOI/TiO_2$ nanotube arrays," *Journal of Physical Chemistry C*, vol. 115, no. 15, pp. 7339–7346, 2011.

[11] Z. H. Xu, J. G. Yu, and G. Liu, "Enhancement of ethanol electrooxidation on plasmonic Au/TiO_2 nanotube arrays," *Electrochemistry Communications*, vol. 13, no. 11, pp. 1260–1263, 2011.

[12] W. B. Zhang, T. C. An, X. M. Xiao et al., "Photoelectrocatalytic degradation of reactive brilliant orange K-R in a new continuous flow photoelectrocatalytic reactor," *Applied Catalysis A*, vol. 255, no. 2, pp. 221–229, 2003.

[13] T. An, G. Li, X. Zhu, J. Fu, G. Sheng, and Z. Kun, "Photoelectrocatalytic degradation of oxalic acid in aqueous phase with a novel three-dimensional electrode-hollow quartz tube photoelectrocatalytic reactor," *Applied Catalysis A*, vol. 279, no. 1-2, pp. 247–256, 2005.

[14] Q. Q. Meng, J. G. Wang, Q. Xie, H. Q. Dong, and X. N. Li, "Water splitting on TiO_2 nanotube arrays," *Catalysis Today*, vol. 165, no. 1, pp. 145–149, 2011.

[15] C. H. Wang, X. T. Zhang, C. L. Shao et al., "Rutile TiO_2 nanowires on anatase TiO_2 nanofibers: a branched heterostructured photocatalysts via interface-assisted fabrication approach," *Journal of Colloid and Interface Science*, vol. 363, no. 1, pp. 157–164, 2011.

[16] L. Gu, F. Y. Song, and N. W. Zhu, "An innovative electrochemical degradation of 1-diazo-2-naphthol-4-sulfonic acid in the presence of $Bi_2Fe_4O_9$," *Applied Catalysis B*, vol. 110, no. 2, pp. 186–194, 2011.

[17] J. Krýsa, G. Waldner, H. Měšťánková, J. Jirkovský, and G. Grabner, "Photocatalytic degradation of model organic pollutants on an immobilized particulate TiO_2 layer. Roles of adsorption processes and mechanistic complexity," *Applied Catalysis B*, vol. 64, no. 3-4, pp. 290–301, 2006.

[18] X. J. Yu, Y. Q. Wang, Z. L. Li, S. Bai, and D. Sun, "Study on deactivated mechanism and regeneration methods of TiO_2 during photocatalytic benzoic acid," *Acta Scientiae Circumstantiae*, vol. 26, no. 3, pp. 433–437, 2006.

[19] Q. Zheng, B. X. Zhou, J. Bai et al., "Self-organized TiO_2 nanotube array sensor for the determination of chemical oxygen demand," *Advanced Materials*, vol. 20, no. 5, pp. 1044–1049, 2008.

[20] J. L. Zhang, B. X. Zhou, Q. Zheng et al., "Photoelectrocatalytic COD determination method using highly ordered TiO_2 nanotube array," *Water Research*, vol. 43, no. 7, pp. 1986–1992, 2009.

[21] D. S. Ling, H. Y. Xie, Y. Z. He, W. E. Gan, and Y. Gao, "Determination of preservatives by integrative coupling method of headspace liquid-phase microextraction and capillary zone electrophoresis," *Journal of Chromatography A*, vol. 1217, no. 49, pp. 7807–7811, 2010.

[22] A. Ali, S. S. Somayeh, and S. Abbas, "Synthesis and antimycobacterial activity of 2-(phenylthio) benzoylarylhydrazone derivatives servicesIranian," *Journal of Pharmaceutical Research*, vol. 10, no. 4, pp. 727–731, 2011.

[23] Z. M. Chen, P. Lu, Y. L. Su, and M. He, "Preparation and performance evaluation of water-based rust inhibitor for iron and steel," *Materials Prodection*, vol. 44, no. 6, pp. 58–59, 2011.

[24] T. Jyothi and C. AKe, "Rasmuson Particle engineering of benzoic acid by spherical agglomeration," *European Journal of Pharmaceutical Sciences*, vol. 45, no. 5, pp. 657–667, 2012.

[25] C. G. Silva and J. L. Faria, "Photocatalytic oxidation of benzene derivatives in aqueous suspensions: synergic effect induced by the introduction of carbon nanotubes in a TiO_2 matrix," *Applied Catalysis B*, vol. 101, no. 1-2, pp. 81–89, 2010.